Full Length Article

Revisitation of FRET methods to measure intraprotein distances in Human Serum Albumin

CrossMark

S. Santini, A.R. Bizzarri, S. Cannistraro *

Biophysics and Nanoscience Centre, Dipartimento DEB, Università della Tuscia, Viterbo, Italy

ARTICLE INFO

ABSTRACT

We revisited the FRET methods to measure the intraprotein distance between Trp-214 (used as donor) of Human Serum Albumin and its Cys-34, labelled with 1.5-Iaedans (used as acceptor). Variation of Trp fluorescence emission in terms of both intensity and lifetime, as well the enhancement of the acceptor fluorescence emission upon Trp excitation, have been monitored. A careful statistical analysis of the fluorescence results from ten independently prepared samples, combined with suitable spectral corrections, provided reproducible distances estimations by each one of the three methods. Even if monitoring of the donor lifetime variation in the presence of the acceptor reproduces at the best the crystallographic data, by allowing even sub-nanometre distance variations to be appreciated, we suggest that a comparative analysis of all the three methods, applied with statistical significance, should be preferred to achieve a better reliability of the FRET technique.

© 2016 Elsevier B.V. All rights reserved.

1. Introduction

Förster Resonance Energy Transfer (FRET) has achieved an increasing success over the years in biological field in which it is used for studying distances, molecular interactions and conformational changes [1–9]. According to Förster theory, excitation of an intrinsic (or extrinsic) fluorescent donor within a molecule may result in energy transfer to a suitable acceptor by means of a non-radiative long-range dipole–dipole coupling. Such an approach has been applied to measure intra- or inter- molecular distances within both immobilized or diffusing samples, both *in vitro* and *in vivo* and even at single molecule level [10–16].

The efficiency of energy transfer (E_{FRET}) from the donor to the acceptor strongly correlates with the distance between them according to an inverse sixth order law; with this implying an accurate measurement of E_{FRET} for reliable distance evaluation. In principle, E_{FRET} can be determined according to the following methods: i) by measuring the donor static fluorescence both in the presence and in the absence of the acceptor; ii) by monitoring the enhancement of the acceptor static fluorescence upon excitation of the donor; iii) by recording the change of the donor lifetime as due to the presence of the acceptor. Although long-lifetime donors, such as lanthanides, which do not require a correction for the acceptor excitation, can be also used [17], generally, it must be ascertained that the recorded fluorescence changes are caused mainly by the energy transfer process from the excited donor to the acceptor. Indeed, the donor fluorescence quenching, which is currently the most widely used method, may be affected by processes other than FRET [4,18]. For instance, the introduction of the acceptor may cause changes (even allosterically) in the donor environment and exposition to the solvent that could, in turn, affect the quenching mechanisms (statically and/or dynamically) [4]. Such a problem could persist even when the change of the donor fluorescence lifetime, which is a method less frequently used, is monitored [19]. All this may result in an over- or under-estimation of E_{FRET} and, consequently, of the donor-to-acceptor (D–A) distance. Actually, only the appearance of the acceptor fluorescence emission, upon excitation of the donor, may specifically indicate the occurrence of a non-radiative energy transfer process [8,18]. However, application of this method could be quite complicated by a possible direct excitation of the acceptor at the donor excitation wavelength; therefore suitable spectral corrections should be applied in order to single out the fluorescence emission as only due to the energy transfer process [8]. Moreover, such a correction requires to use, as a control, the free dye emission which is often subjected to spectral fluctuations as due to several phenomena such as the aggregation of the dye in the ground or excited states, changes of its dipole moment, intramolecular charge transfer, hydrogen bonding between solvent and dye molecules [20]. For all these reasons, such a method is often reported only to demonstrate that energy transfer has occurred, rather than to calculate distances [21,22]. To the best of our

* Correspondence to: Biophysics and Nanoscience Centre, Dipartimento DEB, Università della Tuscia; Largo dell'Università, 01100 Viterbo, Italy. Fax: +39 0761357136.
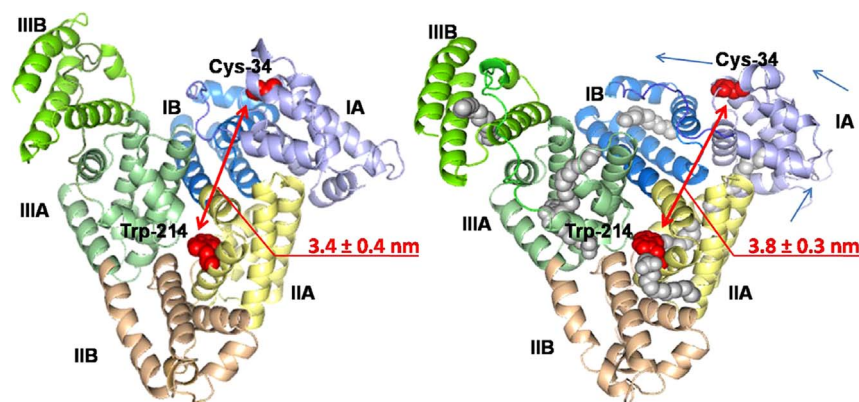*E-mail address:* cannistr@unitus.it (S. Cannistraro).

Fig. 1. Crystallographic structure of HSA [23] at 2.50 Å resolution (A) and of HSA complexed with palmitic acid (B) at 2.43 Å resolution [24]. Trp-214 in sub-domain IIA and Cys-34 in sub-domain IA are represented as red spheres. The distances between the -SH group of Cys-34 and the centre of the Trp-214 indole ring, indicated by a red arrow in both structures, have been measured with the specific pymol wizard. The three structural domains of HSA with their respective sub-domains IA, IB, IIA, IIB, IIIA and IIIB are in the scale of the blue, yellow and green, respectively, both in A and B. Grey spheres in (B) represent palmitic acid molecules while the cyan arrows indicate the direction of domains movement upon palmitic acid binding. (For interpretation of the references to colour in this figure legend, the reader is referred to the web version of this article.)

knowledge, a comprehensive FRET study dealing with a concomitant application of all these three methods and aimed at comparatively determining their reliability and accuracy with statistical significance, is missing.

We have then revisited the measurement of the distance between the lone Trp residue (Trp-214, used as donor) in Human Serum Albumin (HSA) and its lone free Cys (Cys-34), which was labelled with a suitable acceptor dye ((5-({2-[(iodoacetyl)amino] ethyl}amino) naphthalene-1-sulfonic acid, 1.5-Iaedans) (IAD); with such a distance being well known from the HSA crystallographic structure solved at 2.50 Å resolution (Fig. 1A) [23]. All the three FRET methods described have been applied on ten independently prepared samples, to get a reliable statistical significance.

To check the sensitivity of the three methods to appreciate slight protein conformational changes, we have also investigated the D–A distance upon complexing HSA with palmitic acid, which is a long chain fatty acid carried by the protein in the blood plasma [24]. The crystallographic data, which have also been reported at 2.43 Å resolution (Fig. 1B), for this binary system, indicate that HSA undergoes small conformational changes in the presence of palmitic acid, with about 0.4 nm increase of its Trp-214 to Cys-34 distance [24].

Careful experimental design together with rigorous processing of FRET data, and combined with appropriate spectral corrections, allowed us to obtain reproducible distance estimation by means of all the three methods. We found that monitoring of the donor lifetime in the presence of the acceptor results the most accurate and precise FRET method to measure intraprotein distances, even when sub-nanometre distance variations occur. However we suggest that a multi-parameters analysis, based on the application of all the three methods on a statistically significant set of samples, could strongly point out the occurrence of FRET and offer a better reliability for the measurement of distances by FRET.

2. Materials and methods

2.1. Sample preparation

1.5-Iaedans (IAD) was purchased from Molecular Probes. Palmitic acid was from Sigma Aldrich, provided in lyophilized form with a purity degree higher than 99%. HSA from human serum lyophilized powder, essentially globulin free, with a purity degree higher than 99% was purchased from Sigma Aldrich and used without further purification.

For the labelling procedure with the acceptor dye, 15 μM HSA in phosphate buffer (PBS 50 mM pH 7.4) was incubated with twenty fold molar excess of IAD overnight at 4 °C. IAD excess was then removed by extensive dialysis against PBS buffer for 36–48 h and 4 to 6 PBS changes by means of Slide-A-Lyzer™ G2 Dialysis Cassettes (Thermo Scientific) with a cut off of 2000 K. The HSA concentration after dialysis was determined by absorption at 279 nm using a molar extinction coefficient of $36{,}000 \, \text{mM}^{-1} \, \text{cm}^{-1}$ [25]. The amount of bound IAD was determined by the absorption at 337 nm, using a molar extinction coefficient of $5700 \, \text{mM}^{-1} \, \text{cm}^{-1}$ [26]. The protein concentration was corrected for the contribution of IAD at 279 nm and the label stoichiometry was calculated. Typically, the labelling stoichiometry, defined as the moles of dye per mole of protein, was in the range 0.9–1.

Palmitic acid was dissolved in ethanol at a final concentration of 18 mg/ml and successively diluted in PBS buffer. 10 fold molar excess of the resulting solution was then added to the HSA samples. The resulting concentration of ethanol in the HSA final solution was 0.2% v/v, which we observed not to perturb the protein structure [27].

2.2. Spectroscopic measurements and data analysis

Absorbance spectra were recorded at room temperature by a double beam Jasco V-550 UV/visible spectrophotometer by using 1-cm path length cuvettes and 1-nm bandwidth in the spectral region 220–750 nm. Absorbance spectra were collected using PBS buffer as reference.

Steady-state fluorescence measurements were performed with a FluoroMax®-4 Spectrofluorometer (Horiba Scientific, JobinYvon). Samples were excited at 295 nm and fluorescence emission was collected from 305 to 580 nm by using 1 nm increments and integration time of 0.50 s. A 2 nm bandpass was used in both the excitation and emission paths. Spectra were acquired in the signal to reference (S/R) mode to take into account for random lamp intensity fluctuations. Moreover, emission spectra were corrected for Raman contribution from the buffer.

Time-related measurements were performed at room temperature with the time-correlated single photon counting method using FluoroMax®-4 Spectrofluorometer (Horiba Scientific, JobinYvon), operating at a repetition rate of 1 MHz and running in reverse mode. The apparatus was equipped with a pulsed nanosecond LED excitation head at 295 nm (Horiba Scientific, JobinYvon) having a temporal width lower than 1 ns and a bandwidth of 20 nm, which can be reduced by the slits to about 4 nm. Detection

was at 347 nm and the fluorescence lifetime data were acquired until the peak signal reached 10,000 counts.

Time-resolved fluorescence decays were analysed making use of the impulse response function (DAS6 software, Horiba Scientific). The function describing the fluorescence decay was assumed to be a sum of exponential components and data were analysed by employing a non-linear least square analysis including deconvolution of the prompt from Horiba, JobinYvon:

$$I(t) = \sum_{i=1}^{n} a_i e^{(-t/\tau_i)} \tag{1}$$

In which $I(t)$ is the time-dependent intensity, α_i is the pre-exponential factor representing fractional contribution to the time resolved decay of the i_{th} component with lifetime τ_i. The goodness of the fit was judged in term of both χ^2 value and weighted residuals. The fluorescence decay of both HSA and IAD-labelled HSA, both before and after palmitic acid addition, was found to be biexponential, as expected [28]. The average fluorescence lifetime of Trp-214, $\langle \tau \rangle$, was then calculated by:

$$\langle \tau \rangle = \frac{\sum_{i=1}^{n} a_i \tau_i}{\sum_{i=1}^{n} a_i} \tag{2}$$

Förster theory of dipole–dipole coupling was used to estimate distance between HSA Trp-214 and Cys-34; the latter having been covalently labelled with IAD. E_{FRET} from the donor (Trp-214, D) to the acceptor (IAD, A) was obtained by three methods: i) by measuring the quenching of the donor static fluorescence resulting from the presence of the acceptor (the donor static fluorescence quenching method); ii) by the change of fluorescence emission intensity of the acceptor fluorophore consequent to the donor excitation (the enhancement of acceptor fluorescence emission method); iii) by measuring the donor fluorescence emission lifetime changes (the donor lifetime variation method). For each one of these methods, ten independent experiments were performed on independently prepared samples and the ten resulting E_{FRET} values were used to calculate the average D–A distances with their corresponding standard deviations.

In the donor static fluorescence quenching method samples were excited at 295 nm (where the Trp-214 still absorbs, while Tyr and Phe residues are not substantially excited) and the fluorescence emission intensity of D was recorded in both the unlabelled and IAD-labelled HSA samples. The related E_{FRET} was calculated according to:

$$E_{FRET} = 1 - \frac{F_{DA}}{F_D} \tag{3}$$

In which F_D and F_{DA} were the fluorescence emission intensities of D in the absence and the presence of A, respectively [4]; with both having been recorded at 347 nm.

E_{FRET} from the enhancement of the acceptor fluorescence emission was calculated as the ratio of A fluorescence emission at 468 nm in the presence (F_{AD}) and in absence (F_A) of D [4]. This ratio was corrected for the direct excitation of A at the excitation wavelength of 295 nm used to excite D, where IAD shows a significant absorption (Fig. 2). Since the free IAD emission was subjected to significant fluctuations as previously mentioned [20] we cannot use this emission as control. In this respect, we observed that IAD fluorescence emission can be stabilized by the binding to a peptide; we therefore, used as control its fluorescence intensity when bound to a peptide which does not contain Trp residues. The synthetic peptide p29 [29] consisting in the 28 amino acids fragment of the blue copper protein Azurin, p28, modified with an N-ter Cys used for specific labelling with IAD was chosen. For p29 labelling, the same procedure previously described for HSA
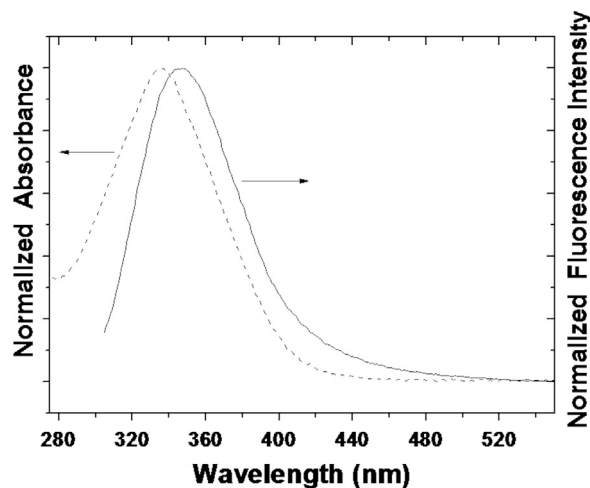

Fig. 2. Spectral overlap between Trp-214 emission spectrum (solid line) and the absorption spectrum of IAD (dashed line) in solution. Emission spectrum was obtained by exciting HSA in 50 mM PBS buffer pH 7.4 at 295 nm wavelength and it was corrected for Raman contribution from the buffer. IAD absorption was recorded in 50 mM PBS pH 7.4 by using buffer as blank.

labelling was followed. The IAD/p29 stoichiometric ratio resulted to be very close to 1. The correction for E_{FRET} calculation by acceptor enhancement was thus performed by subtracting the direct emission of IAD/p29 (F_A) from F_{AD} and then by multiplying for the ratio of the molar extinction coefficient of IAD/p29 (ε_A) and D (ε_D) at the excitation wavelength of 295 nm [4,8,18] according to:

$$E_{FRET} = \left(\frac{F_{AD} - F_A}{F_A}\right)\left(\frac{\varepsilon_A}{\varepsilon_D}\right) = \left(\frac{F_{AD}}{F_A} - 1\right)\left(\frac{\varepsilon_A}{\varepsilon_D}\right) \tag{4}$$

Where F_{AD} has been corrected for the emission intensity of Trp at 468 nm (Fig. 3, dashed line). Finally, the donor lifetime variation method was used to calculate E_{FRET} by using the equation:

$$E_{FRET} = 1 - \frac{\langle \tau_{DA} \rangle}{\langle \tau_D \rangle} \tag{5}$$

where $\langle \tau_{DA} \rangle$ and $\langle \tau_D \rangle$ are the average donor lifetime in presence and absence of A, respectively, and obtained by applying Eq. (2).

The E_{FRET} values provided by each one of the described methods, were finally used to calculate the distance between Trp-214
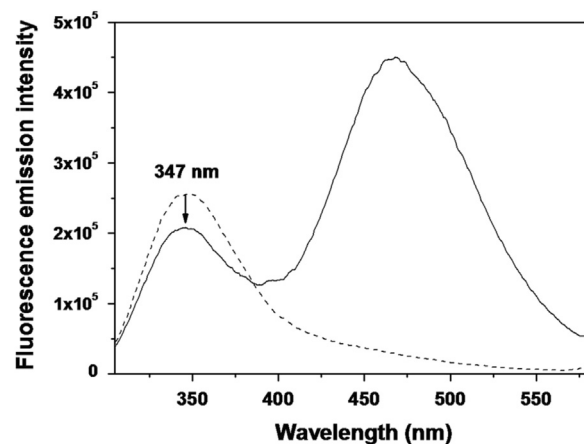

Fig. 3. Representative fluorescence emission spectra of HSA (dashed line) and IAD-labelled HSA (solid line). Spectra were recorded after samples excitation at 295 nm and corrected for Raman contribution from the buffer. The arrow indicates the quenching of Trp-214 emission intensity in IAD/HSA with respect to unlabelled HSA.

and IAD-labelled Cys-34, according to:

$$E_{FRET} = \frac{R_0^6}{R_0^6 + R^6} \qquad (6)$$

The Förster or critical radius R_0 is defined as the D–A distance at which the energy transfer efficiency is 50%. The R_0 value for the Trp-IAD couple is assumed to be 22 Å [2].

HSA figures were created with Pymol (http://www.pymol.org/), a powerful molecular graphics system that has 3D capabilities [30,31].

3. Results and discussions

Fig. 2 shows the emission spectrum of the single tryptophan (Trp-214) of HSA (solid line) when excited at 295 nm, together with the free IAD absorption spectrum (dashed line). The significant spectral overlap clearly indicates that Trp and IAD are a good donor-acceptor couple to be used in FRET experiments [2].

Fig. 3 shows the emission spectrum of unlabelled HSA as resulting from the excitation of its Trp-214 (dashed line) and of IAD-labelled HSA (solid line), in buffer solution. It is evident that the fluorescence emission intensity of HSA, centred at 347 nm, is significantly quenched in the presence of the acceptor, as indicated by the arrow.

By assuming that such a quenching is completely due to the energy transfer process (thus excluding any other possible causes, as mentioned in the Introduction), Eq. (3) is used to obtain E_{FRET} and, in turn, Eq. (6) provides the D–A distance. Table 1 reports the average value of the D–A distance, calculated by this method, on ten independently prepared samples, with the corresponding standard deviation. By comparing the mean value for the Trp-214 to Cys-34 distance with that measured from the HSA crystallographic structure [23] (Fig. 1A also reported in Table 1, last column) we observe that the former is about 0.60 nm shorter. However, if the standard deviations are taken into account, there is some overlap between the FRET and the crystallographic data. The FRET D–A distance is in good agreement with the value of 2.97 ± 0.10 nm measured between Trp-214 and acrylodan labelled Cys-34 [32]; while there is a lesser agreement with the values of 3.18 ± 0.03 nm and of 3.31 ± 0.08 nm found between Trp-214 and Cys-34 labelled with azomercurial [33] and 7-(diethyl amino)-4-methylcoumarin 3-maleimide [34], respectively. Nevertheless, it is not clear if the quite low standard errors reported in these papers derive from independent measurements or are only provided by the fitting procedures.

Fig. 4 shows the emission spectrum of IAD (dashed line) bound to p29 and of IAD-labelled HSA (solid line), excited at 295 nm.

Fig. 4. Representative fluorescence emission spectra of IAD-labelled HSA (solid line) and IAD-labelled p29 (dashed line). Spectra were recorded after samples excitation at 295 nm and corrected for Raman signal from the buffer.

It can be observed that the fluorescence emission intensity of IAD when is bound to HSA is significantly higher than the IAD emission when it is bound to p29, as indicated by the arrow. We carefully verified that the IAD concentration, determined as previously described in Material and method section, was the same in both systems. Moreover we corrected for the direct excitation of IAD, finding that about 25% of the total emission intensity is due to its direct excitation at 295 nm; the remaining fluorescence intensity being due to the energy transfer process. This allowed us to calculate a D–A distance of 3.0 ± 0.2 nm (Table 1); with this value being closer to the crystallographic one (Table 1, last column) than that calculated by using the donor static fluorescence quenching method. By considering the variability of the experimental data, we observe a wider overlap with the crystal structure data than that found by the previous method. To the best of our knowledge there are not literature data with which we can compare our result; indeed the acceptor enhancement in the current literature, is reported only to ascertain that energy transfer has occurred, rather than to quantify distances.

When time-resolved fluorescence emission is followed, the fluorescence decay trends as those shown in Fig. 5 for HSA (grey trace) and IAD-labelled HSA (black trace) were obtained.

By fitting the corresponding decay spectra from ten independent experiments, we obtained a HSA Trp-214 lifetime of $\langle \tau_D \rangle = 5.68 \pm 0.09$ ns, in good agreement with published data [28]. A significant reduction is observed in the presence of IAD ($\langle \tau_{DA} \rangle = 5.12 \pm 0.11$ ns). If we assume that such a quenching is only due to the energy transfer from D to A, Eqs. (5) and (6) give an average D–A distance of 3.2 ± 0.1 nm (see Table 1). This is in a very good agreement with the value of 3.15 ± 0.03 nm found between Trp-214 and acrylodan labelled Cys-34 [35] (also for this paper it is not

Table 1
Trp-214 to Cys-34 distance in HSA.

Sample	Distance (nm)			
	Donor fluorescence quenching	Acceptor fluorescence emission	Donor lifetime variation	Crystal structure
HSA	2.8 ± 0.3	3.0 ± 0.2	3.2 ± 0.1	3.4 ± 0.4
HSA/palmitic acid	3.0 ± 0.2	3.2 ± 0.3	3.5 ± 0.1	3.8 ± 0.3

Distance between Trp-214 and Cys-34 in HSA (third row) and in the HSA/palmitic acid system (fourth row). Reported distances are the average values resulting from ten independent experiments and obtained by using: i) the donor static fluorescence quenching method (second column); ii) the enhancement of acceptor fluorescence emission method (third column); iii) the donor lifetime variation method (fourth column). The last column reports the distances measured on the crystallographic structures [23,24].
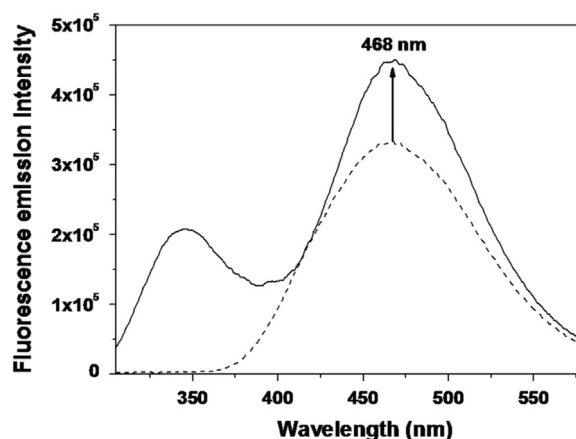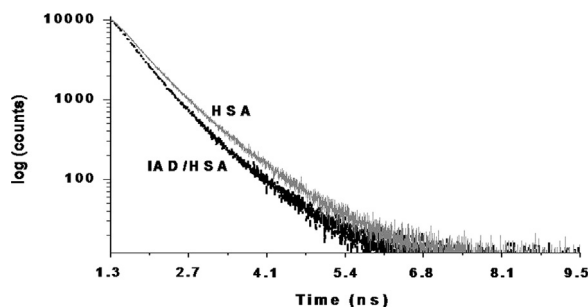

Fig. 5. Representative fluorescence decay of unlabelled (grey trace) and IAD-labelled (black trace) HSA. Proteins were excited with a 295 nm nanoled pulse and emission was collected at 347 nm.
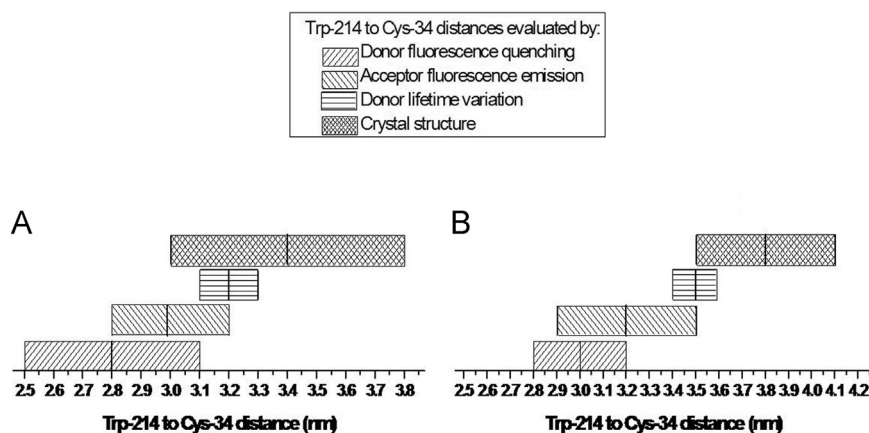
Fig. 6. Comparison of the Trp-214 to Cys-34 distances evaluated by the three methods and measured on the crystal structure of both HSA (A) and HSA/palmitic acid complex (B) with the respective standard deviations. The black line in the middle of each horizontal bar represents the mean value of the distance evaluated by the corresponding method.

clear to infer how the reported quite low error was estimated). This value is the closest to the crystallographic data with respect to those obtained by the two static fluorescence methods. Moreover, by considering the standard deviations, it almost completely overlaps with that coming from the 3D structure of the protein (see Table 1).

To check the sensitivity of each method to appreciate sub-nanometer distance variations, we applied the three methods, with the same statistical analysis, to study the HSA/palmitic acid system. Indeed, from the crystallographic data on this complex it is well known that, upon palmitic acid binding to HSA, he Trp-214 to Cys-34 distance increases of about 0.4 nm [24] as resulting from a rotation of the protein domains as indicated by cyan arrows in Fig. 1B.

The emission and fluorescence decay spectra of both HSA and IAD/HSA in the presence of palmitic acid (not shown) displayed qualitatively the same shape of those shown in Figs. 3–5 for samples without palmitic acid. The average Trp-214 to Cys-34 distances obtained with the three methods are reported in Table 1 (fourth row).

The D–A distance calculated by the donor static fluorescence quenching, was of 3.0 ± 0.2 nm. This value is quite lower (of about 0.8 nm) than that estimated from the HSA/palmitic acid crystal structure [24] (3.8 ± 0.3 nm) (Fig. 1B and Table 1, last column) and there is no overlap between the values of the fluorescence and crystal data. The acceptor fluorescence method provided an average distance (3.2 ± 0.3 nm) closer to the crystal value than that obtained by the previous method; but, again, the variability of the obtained values does not overlap the crystal data. Conversely, the donor lifetime variation method provided a D–A average distance (3.5 ± 0.1 nm) which almost completely overlaps the crystallographic one.

For an easier, visual comparison of the overall results, we have shown the average D–A distances provided by the three methods, together with their standard deviations in Fig. 6A (for HSA) and Fig. 6B (for the HSA/palmitic acid complex). We immediately remark that all the FRET methods always underestimate the Trp-214 to Cys-34 distance inferred by the crystallography, both in free HSA and in the HSA/palmitic acid system. It could be reasonable to attribute this to the peculiar conformation of the solvated protein, likely resulting in a different donor to acceptor distance with respect to the crystallographic structure. It is interesting to remark that such a discrepancy is more evident for the HSA/palmitic acid complex than for free HSA. Two hypothesis could be put forward in this case: i) the donor to acceptor distance in the solvated form of the HSA/palmitic acid system could be quite lower than what observed in the absence of palmitic acid; ii) the palmitic acid

addition could introduce additional relaxation effects leading to higher error in the FRET process. However, since the variability of the average values obtained for the HSA/palmitic acid system are smaller than those obtained from free HSA (at least when the donor static fluorescence quenching and the donor lifetime variation methods are applied), the first hypothesis might be more reasonable.

Concerning the variability of the data related to free HSA, all the three methods gives D–A distance overlapping the crystallographic data. On the contrary, when palmitic acid is added, only data provided by the lifetime variation method overlap the crystallographic distance. This could be due to a less sensitivity to possible static phenomena induced by the palmitic acid addition that, conversely, may affect the static fluorescence measurements. On the other hand, the lifetime variation method is less sensitive to both sample concentrations and cross-talk among channels [18] and, consequently, to possible experimental errors in sample preparations.

4. Conclusions

Three FRET methods (the donor static fluorescence quenching, the enhancement of acceptor fluorescence emission intensity and the donor lifetime variation methods) have been revisited to measure intraprotein distances in Human Serum Albumin and their sensitivity to appreciate small conformational changes upon interaction with palmitic acid has been investigated. A statistical analysis has been performed on the results from ten independent experiments for each method. We have found that the quenching of the donor fluorescence emission intensity, despite being the most used method to measure distances by FRET, is the less accurate. On the other hand, we found that monitoring the variation of the donor lifetime in the presence of the acceptor revealed to be the most accurate and precise method, probably because of its insensitivity to both static relaxation processes and samples concentration. The enhancement of the acceptor fluorescence emission intensity is also quite accurate, even if it requires careful spectral corrections. Our results suggest that all the three methods should be applied for a correct distance evaluation by FRET: the quenching of the donor fluorescence emission intensity could be used to have an estimation of the distance; the enhancement of acceptor emission intensity should be used to confirm that energy transfer has occurred and then the donor lifetime variation method should be applied to exclude possible

errors due to differences in sample concentrations and cross-talk among channels.

By taking advantage from this comprehensive study, it would be interesting to perform in the future a similar analysis to measure inter- rather than intra-protein distances by using a crystallized complex as benchmark.

Author contributions

SS performed research, analysed data, and wrote the paper, ARB contributed analytical tools and wrote the paper, SC designed research and wrote the paper.

Acknowledgements

References

[1] T. Förster, Ann. Phys. 2 (1984) 55 (Translated by RS Knox, Department of Physics and Astronomy, University of Rochester, Rochester, New York, 1984).
[2] P. Wu, L. Brand, Anal. Biochem. 218 (1994) 1.
[3] L. Stryer, Annu. Rev. Biochem. 47 (1978) 819.
[4] J.R. Lakowicz, Energy transfer, in: J.R. Lakowicz (Ed.), Principles of Fluorescence Spectroscopy, 3rd ed.,Springer, New York, 2006, pp. 443–472 (Chapter 13).
[5] V. Fernández-Dueñas, J. Llorente, J. Gandía, D.O. Borroto-Escuela, L.F. Agnati, C. I. Tasca, K. Fuxe, F. Ciruela, Methods 57 (2012) 467.
[6] M. Yengo, L. Berger, Curr. Opin. Pharmacol. 10 (2010) 731.
[7] C. Sinha, K. Arora, C.S. Moon, S. Yarlagadda, K. Woodrooffe, A.P. Naren, Biochim. Biophys. Acta 1840 (2014) 3067.
[8] I. Medintz, N. Hildebrandt, FRET – Förster Resonance Energy Transfer From Theory to Applications, Wiley-VCH Verlag GmbH, Weinheim, 2014.
[9] A. Periasami, R.N. Day (Eds.), Molecular Imaging, FRET Microscopy and Spectroscopy, Academic Press, New York, 2005.
[10] U.B. Choi, K.R. Weninger, M.E. Bowen, Methods Mol. Biol. 896 (2012) 3.
[11] S. Jeganathan, M. Von Bergen, H. Brutlach, H.J. Steinhoff, E. Mandelkow, Biochemistry 452 (2006) 283.
[12] A.A. Deniz, M. Dahan, J.R. Grunwell, T. Ha, A.E. Faulhaber, D.S. Chemla, P. G. Schultz, Proc. Natl. Acad. Sci. USA 96367 (1999) 0.
[13] E. Hirata, H. Yukinaga, Y. Kamioka, Y. Arakawa, S. Miyamoto, T. Okada, E. Sahai, M. Matsuda, J. Cell. Sci. 125 (2012) 858.
[14] R.M. Clegg, Curr. Opin. Biotecnol. 6 (1995) 103.
[15] B. Schuler, H. Hofmann, Curr. Opin. Struct. Biol. 23 (2013) 36.
[16] R. Roy, S. Hohng, T. Ha, Nat. Methods 5 (2008) 507.
[17] F. Morgner, D. Gessler, S. Stufler, N.G. Butlin, H.G. Löhmannsröben, N. Hildebrandt, Angew. Chem. – Int. Ed. 49 (5) (2010) 7570.
[18] P.R. Selvin, Methods Enzymol. 246 (1995) 300.
[19] L.A. Munishkina, A.L. Fink, Biochim. Biophys. Acta 2007 (1768) 1862.
[20] A. Hawe, M. Sutter, W. Jiskoot, Pharm. Res. 25 (2008) 1487.
[21] H.S. Rye, Methods 24 (2001) 278.
[22] I. König, A. Zarrine-Afsar, M. Aznauryan, A. Soranno, B. Wunderlich, F. Dingfelder, J.C. Stüber, A. Plückthun, D. Nettels, B. Schuler, Nat. Methods. 12 (2015) 773.
[23] S. Sugio, A. Kashima, S. Mochizuki, M. Noda, K. Kobayashi, Protein Eng. 12 (1999) 439.
[24] A.A. Bhattacharya, T. Grüne, S. Curry, J. Mol. Biol. 303 (2000) 721.
[25] T. Peters, Adv. Protein Chem. 37 (1985) 161.
[26] D.S. Logvinova, D.I. Markov, O.P. Nikolaeva, N.N. Sluchanko, D.S. Ushakov, D. I. Levitsky, PLoS One 10 (2015) e0137517.
[27] N.E. Basken, C.J. Mathias, M.A. Green, J. Pharm. Sci. 98 (2009) 2170.
[28] L. Yuqin, Y. Guirong, Y. Zhen, L. Caihong, J. Baoxiu, J.C. Jiao, G. Yuron, Biomed. Res. Int. 2014 (2014) 734850.
[29] A.R. Bizzarri, S. Santini, E. Coppari, M. Bucciantini, S. Di Agostino, T. Yamada, C. W. Beattie, S. Cannistraro, Int. J. Nanomed. 6 (2011) 3011.
[30] W.L. DeLano, The PyMOL Molecular Graphics System, 2002. ⟨http://www.pymol.org⟩.
[31] D. Seeliger, B.L. De Groot, J. Comput. Aided Mol. Des. 24 (2010) 417.
[32] J. González-Jiménez, M. Cortijo, Protein J. 23 (2004) 351.
[33] N. Hagag, E.R. Birnbaum, D.W. Darnall, Biochemistry 22 (1983) 2420.
[34] S.S. Krishnakumar, D. Panda, Biochemistry 41 (2002) 7443.
[35] K. Flora, J.D. Brennan, G.A. Baker, M.A. Doody, F.V. Bright, Biophys. J. 75 (1998) 1084.